

Mechanistic Studies on the Reductase Component of *p*-Hydroxyphenylacetate 3-hydroxylase from *Acinetobacter baumannii*.

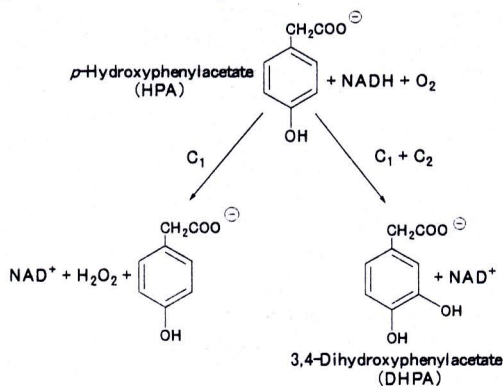
Jeerus Sucharitakul¹, Pimchai Chaiyen¹, Barrie Entsch², and David P. Ballou²

¹ Department of Biochemistry and Center for Excellence in Protein Structure & Function, Faculty of Science, Mahidol University, Rama 6 Road, Bangkok, Thailand, E-mail: jsucharitakul@hotmail.com, Fax: (662)354-7174

² Department of Biological Chemistry, University of Michigan, Ann Arbor, MI, USA.

Introduction

p-Hydroxyphenylacetate (HPA) hydroxylase (HPAH) catalyzes hydroxylation of the substrate *p*-hydroxyphenylacetate (HPA) to 3,4-dihydroxyphenylacetate (DHPA) [1-3]. This hydroxylation reaction is usually found as the initial reaction in the degradation pathway of *p*-hydroxyphenylacetate, one of the major metabolites of lignin [4]. The enzyme HPAH was first purified from *Pseudomonas putida* and was shown to be the two-component enzyme [1]. Studies of *P. putida* HPAH have shown that FAD was tightly bound to the small component and the large component is a coupling protein enabling hydroxylation [1,5]. HPAH from *A. baumannii* is a two-component enzyme composed of a smaller component (C₁) and a larger component (C₂). C₁ is the reductase component generating reduced flavin for the hydroxylase component (C₂), enabling C₂ to hydroxylate HPA. In the absence of C₂, C₁ catalyzes the oxidation of NADH without hydroxylating HPA and produces H₂O₂ as a final product (**scheme 1**) [3]. In the presence of C₂, the reduced flavin bound to C₁ is presumably transferred to C₂ and the reoxidation of flavin occurs concomitantly with the hydroxylation of HPA (**scheme 1**). Reduced flavin generated by photo-reduction can be also used instead of C₂ for hydroxylation and studies showed that a C(4a)-substituted flavin species was involved with the hydroxylation of HPA [3].



In this study, we have investigated the reaction mechanism of the reductase component of HPAH from *Acinetobacter baumannii*. Pre-steady state kinetics and thermodynamics were used in the study. Knowledge obtained could explain the catalytic mechanism of

HPAH and also could suggest mechanistic models for other two-protein component enzymes.

Experimental Procedures

The reductase component was cloned and expressed in *E. coli* BL-21 (DE3). Enzyme was purified as previously published [6].

Determination of molar absorption coefficient of C₁ component

Holoenzyme (20 μ M) in 10 mM sodium phosphate buffer pH 7.0 was recorded absorption spectrum and then, denatured by adding 0.2 %SDS. Concentration of the released FMN was calculated from absorbance value and molar absorption coefficient (ϵ_{446}) of $12.2 \times 10^3 \text{ M}^{-1} \text{ cm}^{-1}$. The molar absorption coefficient of C₁ was calculated based on FMN concentration.

Rapid reaction experiments

Reactions were carried out in 50 mM sodium phosphate buffer, pH 7.0, 4 °C, unless otherwise specified. Rapid kinetics measurements were performed with Hi-Tech Scientific Model SF-61DX or model SF-61SX stopped-flow spectrophotometers in single mixing mode. The stopped-flow apparatus was made anaerobic by flushing the flow system with an anaerobic buffer solution containing glucose and glucose oxidase. For studying the reduction of C₁ by NADH or NADD, enzyme or enzyme-HPA complexes were placed in tonometers and equilibrated with argon or nitrogen [7]. NADH or NADD solutions were placed in glass syringes and made anaerobic by bubbling with oxygen-free argon for 6 minutes before loading onto the stopped-flow machine. For studying the reaction of reduced C₁ with oxygen, anaerobic enzyme solution in a glass tonometer was reduced with a solution of sodium dithionite delivered from a syringe attached to the tonometer. Solutions with various concentrations of oxygen were prepared by equilibrating buffer with air and certified oxygen in nitrogen gas mixtures.

Redox potential determinations

Redox potentials of C₁-bound FMN, in the presence or absence of HPA in 50 mM sodium phosphate buffer, pH 7.0 at 25 °C were determined by the method of Massey [8]. Xanthine and xanthine oxidase were used to catalytically reduce the enzyme with benzyl viologen as an electron mediator. The dye employed as reference potential for determination of redox potential for both C₁ and C₁-HPA complexes was phenosafranine, $E_m^{\circ} = -252 \text{ mV}$ [9]. During the reduction process, absorbance at wavelengths 458 and 512 nm was used to calculate the amount of oxidized enzyme and dye.

Results

Interaction of C₁ with FMN

The binding of C₁ to FMN results in perturbation of absorption spectrum (Figure 1), causing the λ_{max} of the flavin absorption shift to 458 nm. Molar absorption coefficient of holoenzyme was calculated to be $12.83 \times 10^3 \text{ M}^{-1} \text{ cm}^{-1}$. Using an ultrafiltration unit (Centricon) to determine the amount of free FMN released from the holoenzyme, the K_d of C₁-FMN complex was calculated to be 0.01 μ M, indicating that apoC₁ binds tightly to FMN.

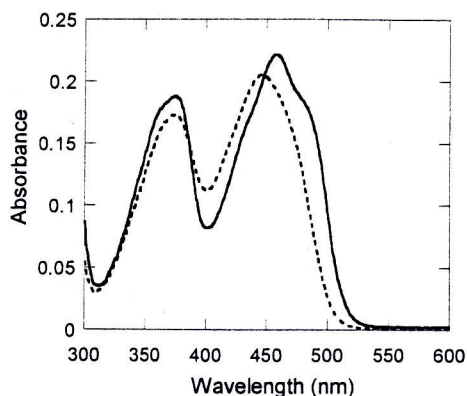


Fig 1: Spectrum of C₁. C₁ (20 μM) was shown in the solid line. After adding 0.2% SDS to the enzyme, the spectrum was shown in the dotted line.

Reductive-half reaction of free enzyme

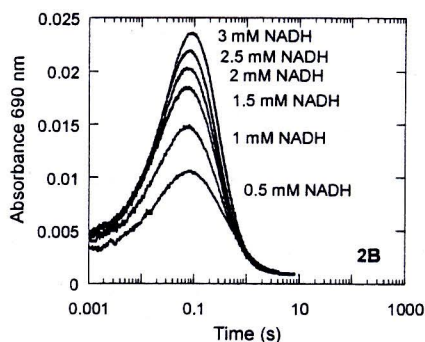
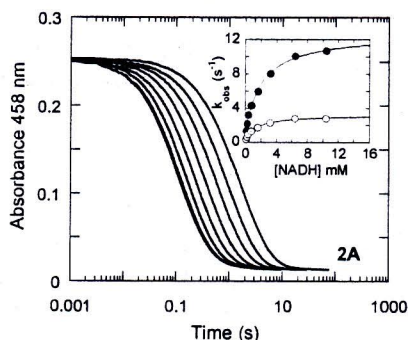
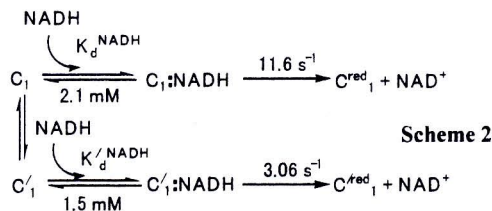


Fig 2A: Kinetic traces for the reduction of C₁. Reduction of C₁ (20 μM final) by NADH (0.1, 0.2, 0.4, 0.8, 1.6, 3.2, 6.4, and 10.4 mM after mixing) in 50 mM sodium phosphate buffer, pH 7.0, 1 mM DTT and 0.5 mM EDTA at 4 °C was monitored in the stopped-flow spectrophotometer at 458 nm. Traces from right to left are from lower to higher concentrations of NADH. Data were fitted with two exponentials. Inset to the figure 2A shows that both rate constants (k_{obs}) are hyperbolically dependent on NADH concentration.

Fig 2B: Charge-transfer complex in C₁ reduction. The reaction was performed in the condition similar to in Figure 2A, but different in NADH concentration and monitored at 690 nm. Analysis has shown that the traces consist of three kinetic phases. The first phase ($k_{\text{obs}} \sim 33 \text{ s}^{-1}$) was an increase in absorbance and independent of NADH concentration. The second and third phases are the decrease in absorbance with k_{obs} of $\sim 3.7 \text{ s}^{-1}$ and $\sim 0.8 \text{ s}^{-1}$, respectively.

The reduction of free enzyme by NADH resulted in biphasic kinetic. At the lowest NADH concentration, the faster phase accounts for $\sim 50\%$ of the total change whereas at higher NADH concentration, the amplitude of the faster phase is around 80% of the total change. The reaction was described as model described in **Scheme 2** where the enzyme exists in two distinct forms.



Reduction of C₁:HPA complex by NADH and NADD

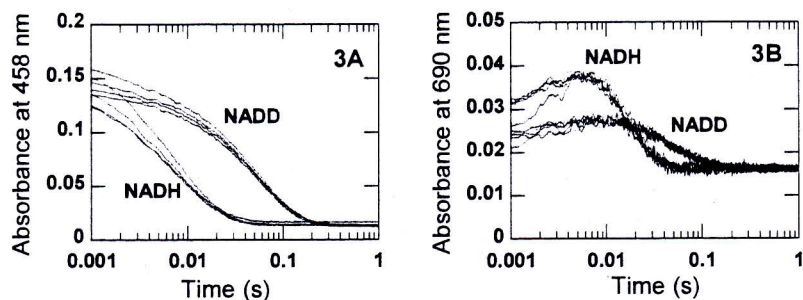
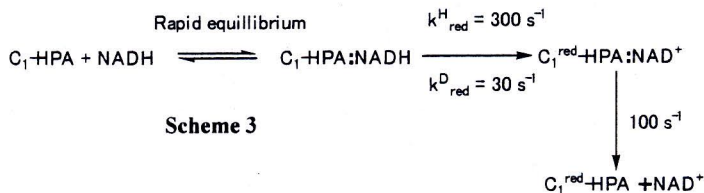


Fig 3A: Kinetic traces of the reduction of the C₁-HPA complex by NADH (NADD) at 458 nm. Enzyme (16 μM) plus 400 μM HPA was mixed with NADH or 4S-NADD at concentrations of 80 μM, 160 μM, 320 μM, and 640 μM (All concentrations were after mixing.). The reactions were performed in 50 mM sodium phosphate buffer pH 7.0 at 4 °C, and monitored at 458 nm. **Fig 3B:** Charge-transfer complex from reduction of C₁-HPA complex. The reactions were the same as in Figure 3A, but monitored at 690 nm.

The reduction of C₁ in presence of HPA is markedly stimulated. At the highest NADH (10.4 mM), free enzyme reduction was finished at 1 s (Figure 2A) whereas in presence of HPA, the reduction was finished at 0.02 s (Figure 3A). Figure 3B indicated that the charge-transfer complex was initially formed during the dead time (the first phase). The second phase (~1-10 ms) is the hydride transfer step indicated by a small increase in absorbance at 690 nm and major decrease in absorbance at 458 nm. The third phase is the decay of the charge-transfer complex with the decrease in absorbance at both wavelengths, 458 and 690 nm. The model describing this reaction is shown as in **Scheme 3**. According to this model, there are two types of charge-transfer complexes, C₁^{ox}:NADH complex forming during the dead time and C₁^{red}:NAD⁺ complex forming during the second phase. The reduction with NADD has shown the kinetic isotope effect of ~ 10 and indicated that the second phase is the hydride transfer step.



Reaction of reduced C_1 with oxygen

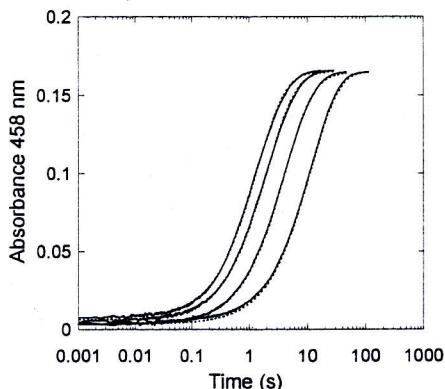
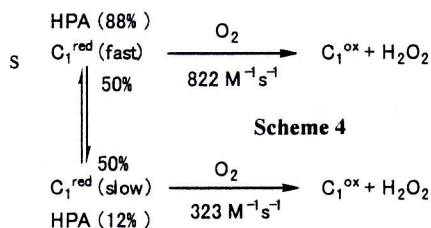


Fig 4: Oxidative half-reaction of the reduced C_1 -HPA complex. Reduced C_1 (16 μM final) with 200 μM HPA (final) was mixed with buffer containing various final oxygen concentrations of 130, 325, 650, and 960 μM (from right to left) in 50 mM sodium phosphate buffer pH 7.0 at 4 $^\circ\text{C}$. All reactions contained catalase (0.3 U) and superoxide dismutase (0.2 U). The reactions were monitored at 458 nm in a stopped-flow spectrophotometer. Dotted lines overlaid are fitted traces for rate constant determination.

The reaction of reduced C_1 and oxygen was investigated by using stopped-flow spectrophotometry in the presence and absence of HPA. Traces of the reaction in presence of HPA were bi-phasic and both phases were comparable in amplitude. The faster phase accounted for 88% of total amplitude change while the rest was accounted for the slower phase. In the absence of HPA, the reaction is also bi-phasic and the amplitude of the each of phase is $\sim 50\%$. The results suggest that the enzyme exists as two isoforms, each reacting to oxygen with different kinetics as shown in **Scheme 4**.



Determination of C_1 reduction potential

	E_m^0 (mV)
FMN	-219
C_1	-236
C_1 -HPA	-254

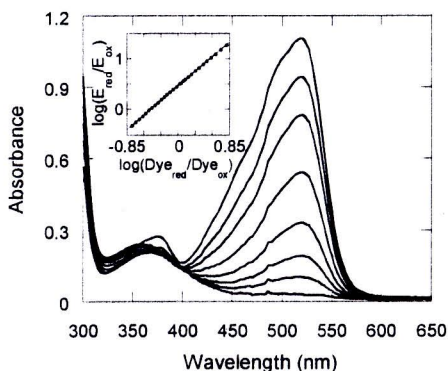


Figure 5: Redox potential determination. Enzyme (23 μ M) and phenosafranine (23 μ M) in 50 mM sodium phosphate buffer, pH 7.0, 25 °C, was slowly reduced by the xanthine/xanthine oxidase system (400 μ M xanthine, 0.01 U xanthine oxidase and 5 μ M benzyl viologen). The reaction was followed spectrally for 6 hours and absorbance values at 458 and 521 nm were used to calculate the amount of oxidized dye and enzyme at different times (Materials and Methods). Inset to the figure shows that the plot of $\log(E_{\text{red}}/E_{\text{ox}})$ versus $\log(\text{Dye}_{\text{red}}/\text{Dye}_{\text{ox}})$ yielded a slope of 1 (Overlaid line is a linear fit with a slope of 1). The redox potential value was calculated to be -236 mV. The redox potential of substrate bound enzyme was shown in table 1.

Conclusion

Stopped-flow studies in both reductive and oxidative half-reaction have showed that C_1 exists as a mixture of isoforms which each form has different reactivity toward reduction and oxidation. In presence of HPA, the reduction of C_1 by NADH was largely enhanced and kinetics appears to be monophasic. In the oxidative half-reaction, when HPA was included, majority of C_1^{red} was in the more reactive form. Data from redox potential measurement indicated that the stimulation by HPA is not resulted from thermodynamic properties since the C_1 -bound FMN has lower E_m^0 value in presence of HPA.

References

1. Arunachalam, U., Massey, V., and Vaidyanathan, C. S. (1992) *J. Biol. Chem.* **267**, 25848-25855.
2. Prieto, M. A., Diaz E., and Garcia, J. L. (1996) *J. Bacteriol.* **178**, 111-120.
3. Chaiyen, P., Suadee, C., and Wilairat, P. (2001) *Eur. J. Biochem.* **268**, 5550-61.
4. Dagley, S. (1987) *Annu. Rev. Microbiol.* **41**, 1-23
5. Arunachalam, U., Massey, V., and Miller, S. M. (1994) *J. Biol. Chem.* **269**, 150-155.
6. Thotsaporn, K., Sucharitakul, J., Wongratana, J., Suadee, C., and Chaiyen, P. (2004) *Biochim. Biophys. Acta.* **1680**, 60-66.
7. Williams, C. H. J. R., Arscott, L. D., Matthews, R. G., Thorpe, C., and Wilkinson, K. D. (1979) *Methods Enzymol.* **62**, 185-198.
8. Massey, V. (1991) *Flavins and Flavoproteins* (Curti, B., Rochi, S., and Zanetti, G., Eds.) pp 59-66, Water DeGruyter & Co., Berlin, Germany.
9. Loach, P. A. (1973) *Handbook of Biochemistry Selected Data for Molecular Biology* (Sorber, H. A., Ed.) pp J-33-J-40, The Chemical Rubber Co., (CRC Press), Cleveland, Ohio.

Table sample

Key words:

p-Hydroxyphenylacetate 3-hydroxylase
two-component enzyme

reductase

p-Hydroxyphenylacetate

FMN